AIAA JOURNAL
Vol. 39, No. 2, February 2001

Unstructured Method for Flows past Bodies in General Three-Dimensional Relative Motion

K. P. Singh* and Oktay Baysal†
Old Dominion University, Norfolk, Virginia 23529

A three-dimensional methodology was developed for unsteady flows past bodies that are in relative motion and where the trajectory of the motion was determined from the instantaneous aerodynamic field. This method coupled the equations of fluid flow and those of rigid-body dynamics and then captured the unsteady aerodynamic interference between the stationary and moving boundaries. The time-dependent, compressible Euler equations were solved on dynamic, unstructured meshes by an explicit, finite volume, and upwind method. The grid adaptation was performed within a window placed around a moving body. The Euler equations of dynamics were then solved by a Runge–Kutta integration scheme. The flow solver and the adaptation scheme were validated by simulating the transonic, unsteady flow around a wing undergoing a forced, periodic pitching motion and then comparing the results with the experimental data. Finally, the overall methodology was demonstrated by simulating the unsteady flowfield and the trajectory of a store dropped from a wing. The methodology, with its computational cost notwithstanding, has proven to be accurate, automated, easy for dynamic gridding, and relatively efficient for the required work hours.

Nomenclature

a_t	=	contravariant speed of cell face
a_∞	=	freestream speed of sound
C_p	=	pressure coefficient
d	=	store diameter
$\boldsymbol{E}$	=	flux vector
$\boldsymbol{F}$	=	body force in inertial frame
$\boldsymbol{g}$	=	gravitational acceleration
I	=	moment of inertia
k	=	reduced frequency
M_∞	=	freestream Mach number
m	=	mass
$\hat{n}(n_x, n_y, n_z)$	=	outward unit normal
p	=	pressure
$\boldsymbol{Q}$	=	flux of conserved flow variables
$\boldsymbol{r}$	=	position vector in noninertial frame
t	=	time normalized by (d/a_∞)
u, v, w	=	components of velocity in inertial frame
$\boldsymbol{V}_{cg}$	=	velocity of center of gravity in inertial frame
$\boldsymbol{V}_r$	=	velocity vector in noninertial frame
x_t, y_t, z_t	=	components of absolute cell face speed
α	=	magnitude of pitching motion
$\boldsymbol{\omega}$	=	angular velocity vector in inertial frame

Introduction

COMPUTATIONAL fluid dynamics has reasonably matured for steady flows. However, there is a strong need for advancements to compute unsteady flows and, subsequently, the flows involving moving bodies. In simulating a flowfield involving a multicomponent configuration, with one or more components engaged in a relative motion, there are at least four levels of assumptions that can be made for the incident-flow and solid-surface interaction.[1] These are as follows: 1) All of the moving components are assumed to be instantaneously frozen, and at each instant, a steady-state computation is performed. 2) All of the moving components are assumed to be engaged in the same rigid-body motion, and the entire computational mesh is assigned this motion during the unsteady flow analyses.[2] 3) Each moving component is assigned its own rigid-body motion, which is either prescribed or it is assumed to be known, so that the motion is input to the unsteady flow computations.[3–7] 4) Beyond and above level 3, the trajectory is determined from the instantaneous flowfield, which is aerodynamically determined.[8–12]

For certain class of relative-moving-body problems, levels 1–3 may be unacceptably compromising. Currently, there appear to exist two different approaches at level 4: dynamic domain decomposition method[3,4,8] and dynamic unstructured technique (DUT).[10–12] The objective of the present paper is to report the latter method's extension for three-dimensional flows with six-degree-of-freedom (DOF) body and boundary motion. The flowchart of DUT is presented in Fig. 1. After a brief description of the method, its validation case will be discussed. The paper will be concluded following the presentation of the computed store separation case.

Synopsis of Methodology

The three-dimensional, time-dependent Euler equations for fluid flow, expressed in the integral form for a bounded domain Ω with a boundary $\partial\Omega$:

$$\frac{\partial}{\partial t}\int_\Omega \boldsymbol{Q}\,\mathrm{d}V + \int_{\partial\Omega} \boldsymbol{E}(\boldsymbol{Q})\cdot\hat{n}\,\mathrm{d}S = 0 \tag{1}$$

were considered. For these dynamic meshes, the contravariant speed of a cell face was written as

$$a_t = x_t n_x + y_t n_y + z_t n_z \tag{2}$$

and the velocity vector of a fluid particle was written relative to the motion of the mesh:

$$\boldsymbol{V}_r = \{(u - x_t), (v - y_t), (w - z_t)\} \tag{3}$$

Second-order spatial discretizations were obtained for either Roe's flux-difference splitting or van Leer's flux-vector splitting. For moving meshes, the contravariant face speed and the contravariant particle velocity relative to the moving mesh [Eqs. (2) and (3)] were used to modify the Roe averaged contravariant velocities and the van Leer defined split fluxes. The solutions at the cell centers were Taylor-series expanded to each of the faces of a tetrahedral cell. The spatially discretized form of the governing equations were then integrated in time using the explicit four-stage Runge–Kutta method. For Eq. (1),

Received 8 February 1996; revision received 9 September 1997; accepted for publication 4 August 2000.

*Graduate Research Assistant, Aerospace Engineering Department; currently Database Analyst, Ohio Savings Bank, Cleveland, OH 44114.

†Professor, Eminent Scholar, and Associate Dean, College of Engineering and Technology; obaysal@odu.edu. Associate Fellow AIAA.

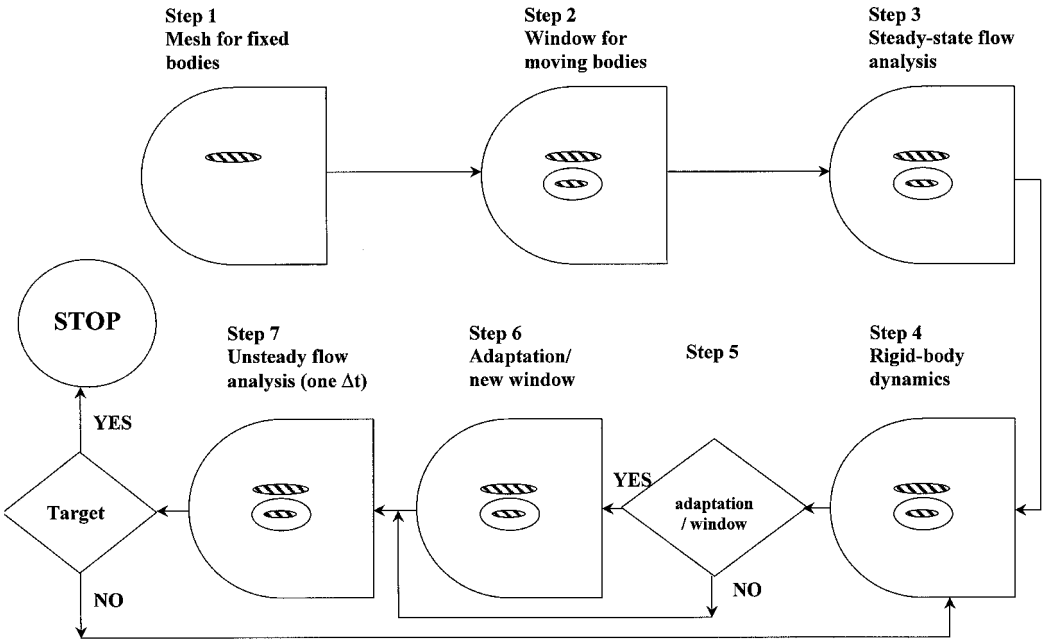

Fig. 1 Flowchart of the present three-dimensional DUT.

this method had a second-order temporal accuracy. To avoid grid-motion induced error, the geometric conservation law had to be satisfied concurrently with the conservation equations.[2,13,14] For the boundary conditions for the present moving boundary problems, the standard inviscid conditions on the wall were adjusted to account for the boundary velocities using the grid speed [Eq. (2)] and for the nonzero pressure gradient using the normal momentum equation [Eq. (1)]. In the far field, characteristic boundary conditions were employed based on the locally one-dimensional Riemann invariants. Detailed discussions of the three-dimensional, steady flow solution algorithm on stationary grids was given by Frink,[15] and the two-dimensional, unsteady flow algorithm on dynamic meshes was reported by Singh et al.[10] and Singh and Baysal.[11]

For the adaptation of the mesh to the boundary motion, the tension-springs analogy was used, where each edge of a tetrahedron represented by a tension spring. Assuming the spring stiffness is inversely proportional to the edge length, the equilibrium of the composite spring forces provided the displacement of each node. To restrict the size of the adaptation region, a window was created around a moving body. The entire domain was searched to locate the nodes that fell within the window (window points) and those that were connected to the outermost window points (frame points). The window points were allowed to be adapted; however, the nodes exterior to the window and the frame points were spatially fixed in time. For problems in which the body had a small or no translational movement, creation of the window took place only once. Otherwise, the window would be constructed at several instants along the path of the body's motion.

Coupled in the overall solution algorithm (Fig. 1) were the governing equations of rigid-body dynamics, used to determine the six-DOF trajectory of a body from a given flowfield:

$$m\frac{\partial \boldsymbol{V}_{\text{cg}}}{\partial t} = \sum \boldsymbol{F} = m\boldsymbol{g} - \int_{\Omega} p\hat{n}\,\mathrm{d}\Omega \tag{4}$$

$$I\frac{\partial \boldsymbol{\omega}}{\partial t} + \int_{\Omega} (\boldsymbol{\omega}\cdot\boldsymbol{r})\cdot(\boldsymbol{r}\times\boldsymbol{\omega})\,\mathrm{d}\Omega = \sum \boldsymbol{r}\times\boldsymbol{F} \tag{5}$$

The present solution method for Eqs. (4) and (5) and its validation were previously presented by Singh et al.[10] and Singh and Baysal.[11] For this purpose, the quasi-steady wind-tunnel data[16] for the separation of a store from a wing were used. These experimentally determined aerodynamic forces and moments were also used as the input to the present dynamic computations. Then the computed

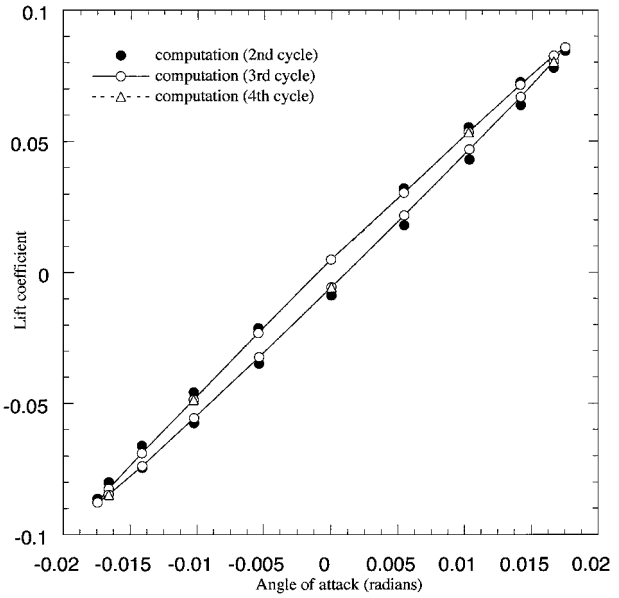

Fig. 2 Limiting cycle for the oscillating rectangular wing case plotted in counterclockwise direction.

store trajectory[10] was successfully compared with the experimental trajectory.[16]

For the harmonic motion considered in the validation case, the pressure coefficient histories computed in the time-domain were Fourier decomposed into their real and imaginary components:

$$\begin{matrix}\text{Re}\\ \text{Im}\end{matrix}\{C_p\} = \frac{2}{\alpha(t_2 - t_1)}\int_{t_1}^{t_2}\left[C_p(\tau)\cdot\left\{\begin{matrix}\sin\\ \cos\end{matrix}(M_\infty k\tau)\right\}\mathrm{d}\tau\right] \tag{6}$$

to distinguish the in-phase from the out-of-phase pressures[17] for the cycle time $t_2 - t_1$. The results will be presented next.

Computational Results

The present methodology was intended and, hence, demonstrated for a multibody configuration in relative motion. First, its validation was attempted using a case for which credible experimental data existed. A rectangular half-span wing, with NACA 64A010 airfoil section and a complete aspect ratio of 4, was placed in Mach 0.8 flow (slightly supercritical) at zero incidence and then subjected

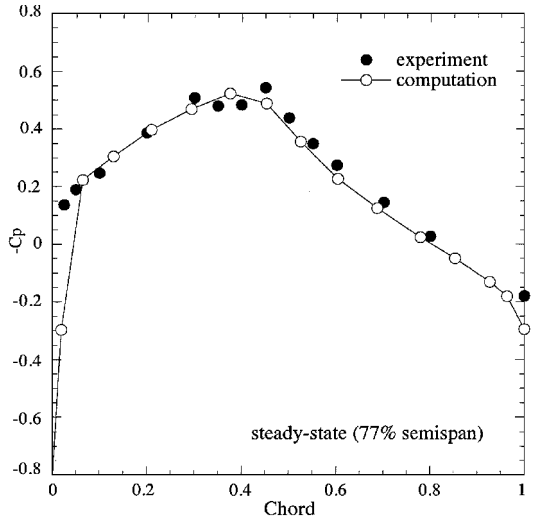

a) 77% semispan, steady state

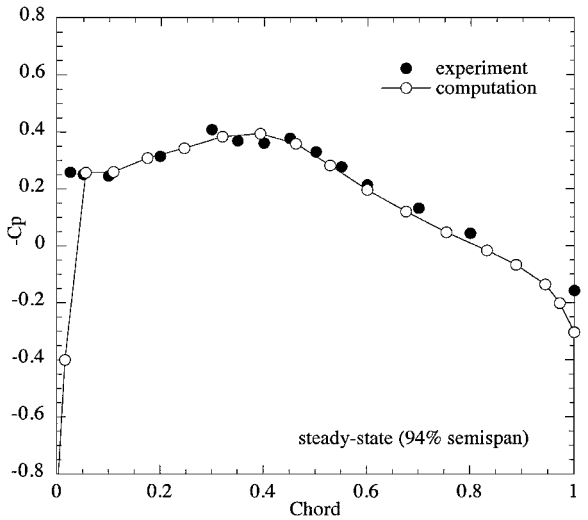

b) 94% semispan, steady state

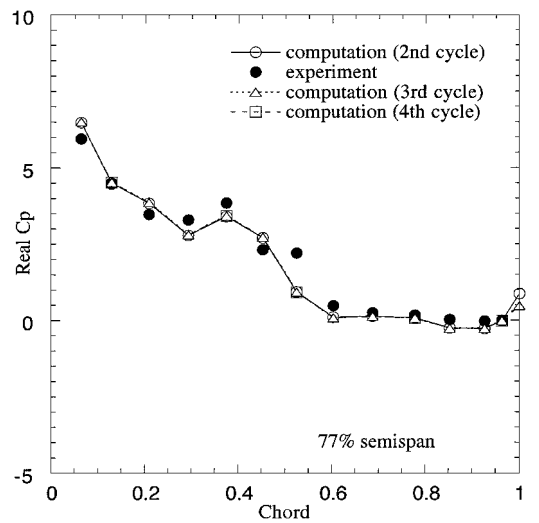

c) 77% semispan, oscillating wing, real C_p

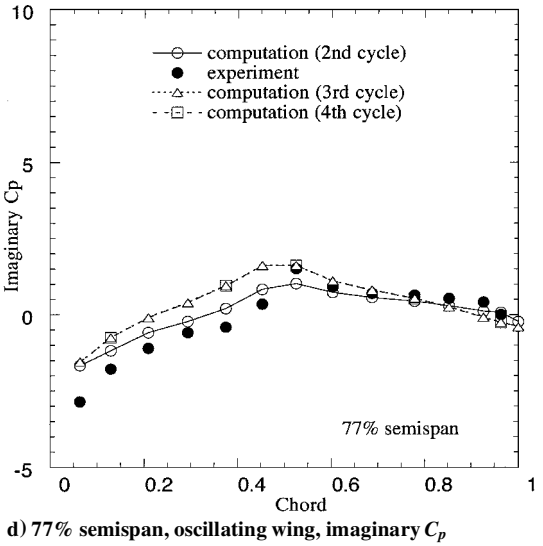

d) 77% semispan, oscillating wing, imaginary C_p

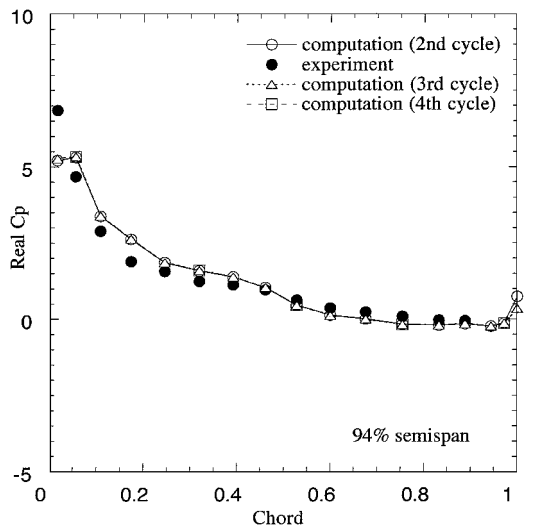

e) 94% semispan, oscillating wing, real C_p

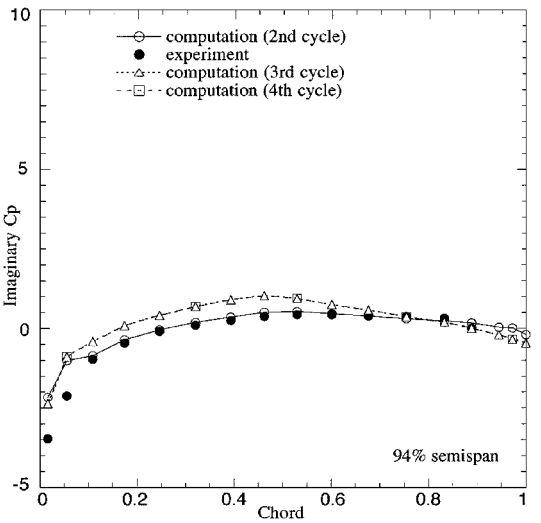

f) 94% semispan, oscillating wing, imaginary C_p

Fig. 3 Comparison of chordwise pressure coefficients for the oscillating rectangular wing.

to a forced, sinusoidal, pitching motion.[17] The amplitude and the reduced frequency of the motion were 1 deg and 0.27, respectively. The unstructured mesh generated for this wing (covered 12 chord lengths both normally and chordwise, and 4 chord lengths spanwise) had 40,533 cells and 7,775 nodes. After obtaining the initial steady-state solution, time-accurate calculations were performed for four cycles. Because the results from the third and the fourth cycles were indistinguishably coincident, the third cycle was deemed as the limiting cycle (Fig. 2).

Comparisons of the present computations, for the steady-state (Figs. 3a and 3b) and unsteady flows (Figs. 3c–3f), with the data (two spanwise stations presented, one supercritical and one fully subsonic critical) were by and large successful. Some discrepancy in the out-of-phase pressures was observed, even among the second and third cycle computations. This was attributed to a number of factors: 1) pressure oscillations with differing phases on upper and lower surfaces, 2) overprediction by the inviscid equations, 3) relatively coarse grid resolution in shock-excursion region, 4) discrepant representation of the wing tip between computation (round) and experiment (flat), and 5) the truncation error. Present results were obtained on a Cray Y-MP computer using 48 MB of memory, and 0.5 and 7.7 CPU hours for steady flow and 1 cycle of unsteady flow computations, respectively. The corresponding unit processing times were about 17 and 42 μs per time step per cell, respectively. Among the observations made in comparison with the implicit, structured, domain-decomposition methods (at level 3 by Chaderjian and Guruswamy[18] and at level 4 by Yen and Baysal[8,14]), the following were deemed noteworthy: 1) The present method did not compromise the second-order temporal accuracy because no time linearization, or approximate factorization, or diagonalization, or interpolations were necessary. 2) A lower number of cells was needed in the present mesh (about one-fifth). 3) This advantage was, however, offset to a certain extent by the smaller time step (about 20 times) required in the present explicit time-marching scheme. The last point was later addressed in Ref. 19.

Next, the present method was demonstrated using a wing-and-store configuration (Fig. 4), which was derived by simplifying the wing–pylon–fin–store configuration given by Heim.[16] It consisted of a clipped delta wing with a 45-deg leading-edge sweep and NACA-64A010 airfoil sections, and directly below this wing, an ogive–cylinder–ogive store. Both the wing and the store were at 0-deg yaw and angle of attack. The oncoming freestream Mach number was 0.95. A computational domain spanning $60d \times 16.5d \times 60d$ in the three directions, respectively, was covered by a relatively coarse unstructured mesh, with 115,864 cells and 21,515 nodes. The adaptation window placed around the store included less than 30% of the total cells, hence, reducing the computational task. For the rigid-body dynamics, the store's mass, normalized by $\rho_\infty d_f^3$, was 8016.2; weight, normalized by $\rho_\infty a_\infty^2 d_f^2$, was 0.43; and the nonzero elements of its moment of inertia tensor, normalized by $\rho_\infty d_f^5$, were $I_{\text{roll}} = 1032.8$, $I_{\text{pitch}} = 18{,}591.9$ and, $I_{\text{yaw}} = 18{,}591.9$, where $d_f = 20d = 0.508$ m, $\rho_\infty = 0.776$ kg/m^3, and $a_\infty = 322.3$ m/s. The impulsive ejection force was 102.4 (intentionally exaggerated by 40 times for a quicker plunge) and was applied until $0.1d$ drop was attained.

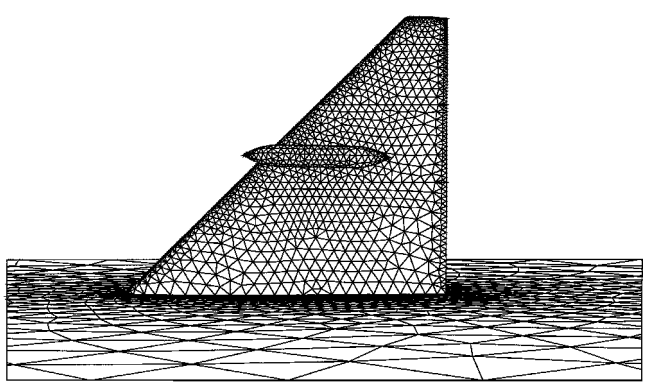

Fig. 4 Surface mesh for the store in carriage position near a delta wing.

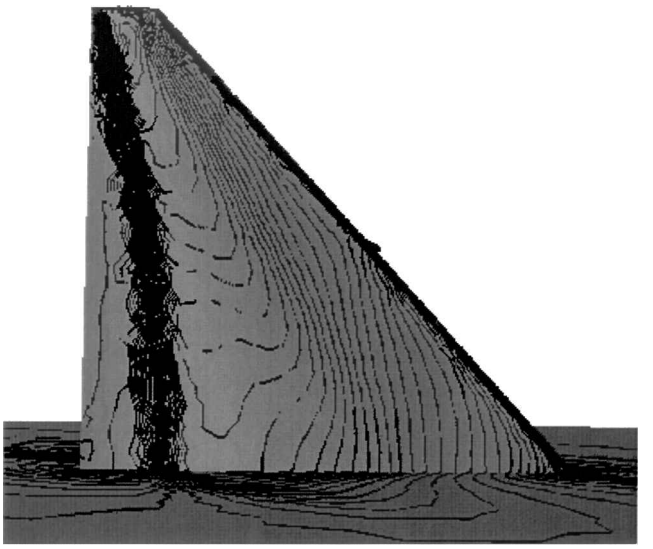

Upper wing surface

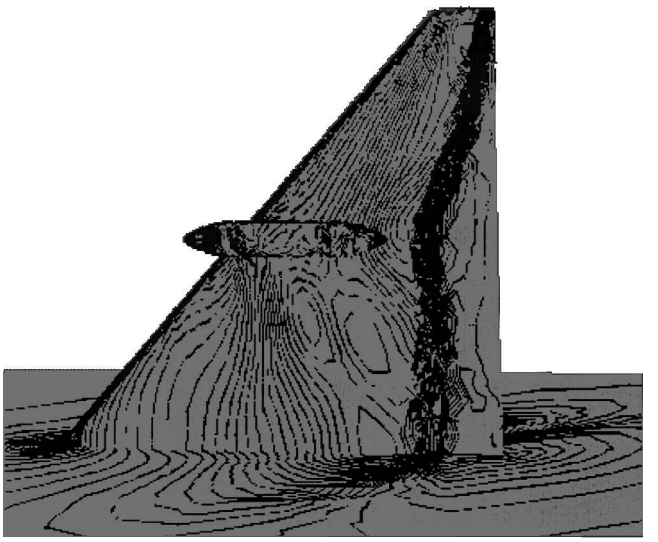

Lower wing surface

Fig. 5 Normalized pressure contours of steady flow at carriage position.

First, the steady-state solution was obtained for the carriage position using local time steps for computational efficiency. The normalized pressure contours for the wing and store surfaces are presented in Fig. 5. Then the computations were continued using time-accurate (global) steps of 1E–3 normalized time units, with corresponding maximum Courant number of about 3. The unsteady flow after $2t$ of separation (store dropped $0.65d$) is shown via its instantaneous pressure contours (Fig. 6). As compared to the carriage position, there were hardly any differences on the upper surface flow (hence upper surface not shown). However, the dynamic, mutual interference manifested itself in a time-varying footprint of the store on the wing's lower surface. This time-dependent effect was more accentuated on the store, as evidenced by the pressure coefficient distributions on the store surface (Fig. 7). The pressure difference between the upper and lower surfaces at $2t$ was much larger than it was at carriage position. This was attributed to the following. First, the pitching down of the store resulted in elevated lower-surface pressures, and second, the widening gap between the store and the wing diminished the interference effect.

The computed six-DOF trajectory for the store's center of gravity is shown in Fig. 8 via its linear displacement and Euler angles. The translational motion was mainly in the downward direction, but small displacements were also observed toward the aft and the

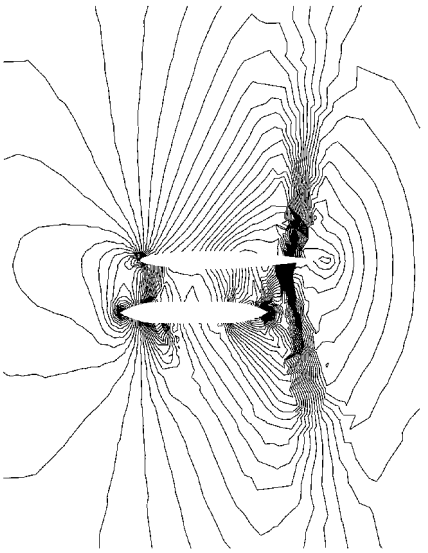

Vertical symmetry plane of the store

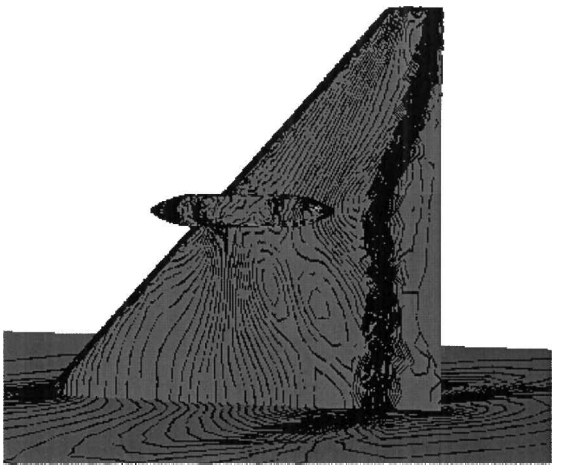

Lower wing surface

Fig. 6 Store separating from a delta wing; contours of normalized instantaneous pressure at time 2*t*.

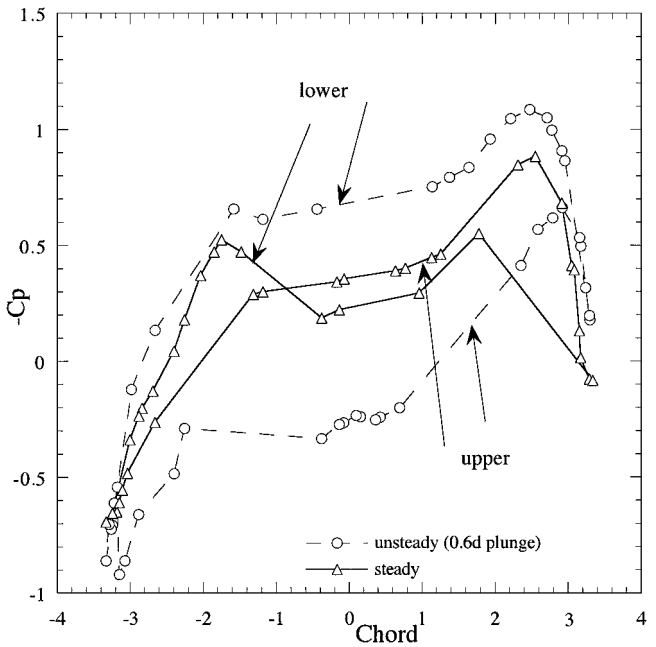

Fig. 7 Instantaneous pressure coefficient distributions on the store: steady-state vs unsteady at time 2*t* (0.65*d* separation). Chord refers to the store length normalized by its diameter.

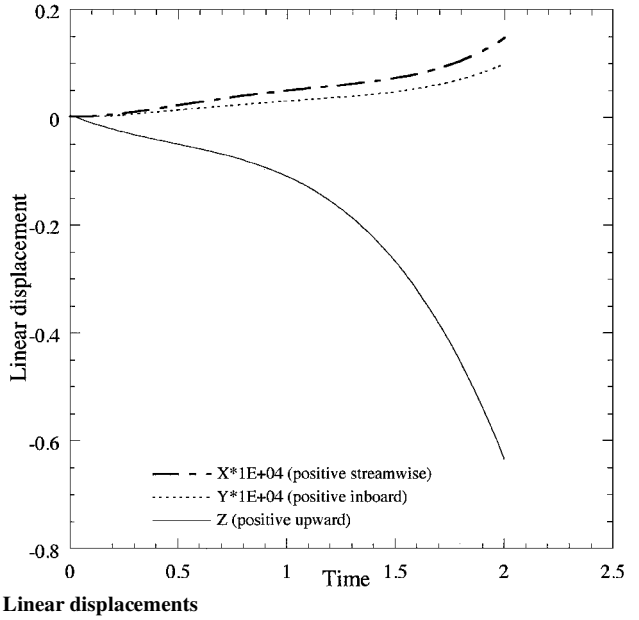

Linear displacements

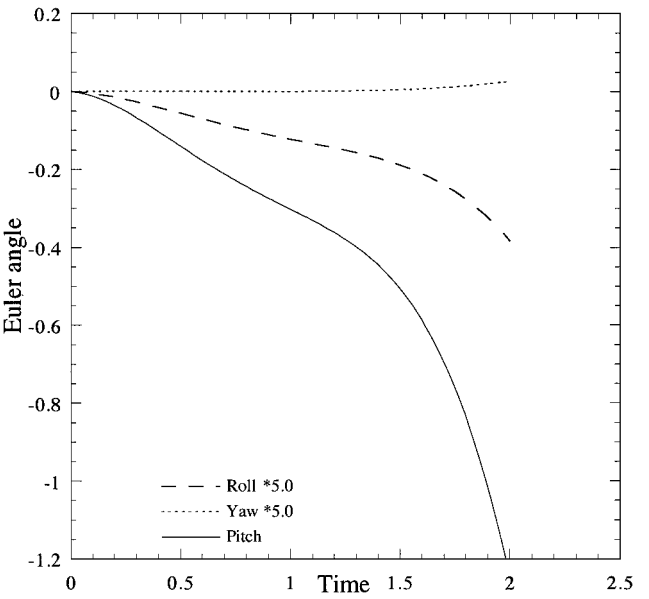

Euler angles

Fig. 8 Trajectory of the store's center of gravity as it separates from a delta wing.

wing root. The store's nose pitched down with a gradual yawing toward the wing outboard. The sideslip and rolling were not quite expected for this axisymmetric store. However, possibly due to the wing-tip effect and the impulsive ejection, some nonsymmetry was introduced into the flowfield. The unsteady load histories (obtained by pressure integration only) resulting from the store motion are shown in Fig. 9. The normal force changed direction abruptly as the ejection force was lifted and kept on increasing. The magnitudes and the temporal changes of the axial and side forces were small. The moments also displayed relatively small temporal changes, but their magnitudes were appreciable and quite disparate. A finite value of the rolling moment was observed, which might be largely due to an error in integrating the pressures on the store. The coarseness of a surface grid could easily result in the numerical directions of the pressures being skewed from the center-line. Finally, the present dynamic simulation on a Cray Y-MP computer for 2*t* and 0.65*d* required 8.3 CPU hours (including 1.64 h for steady-state solution) and 134 MB of memory. The unit processing time for the method was 21 and 42 μs per time step per cell for steady and moving-boundary computations, respectively.

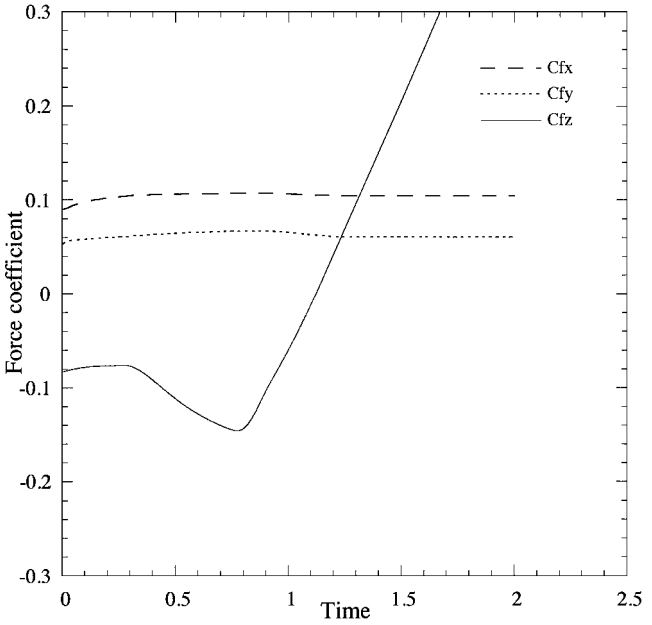

Force coefficients at the center of gravity

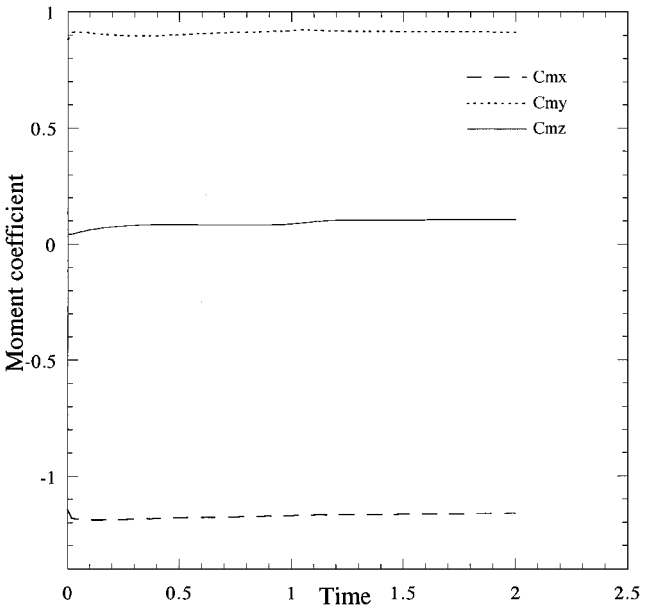

Moment coefficients about the center of gravity

Fig. 9 Unsteady loads on the store as it separates from a delta wing.

Conclusions

A three-dimensional, unstructured-mesh technique was developed to simulate unsteady flows past bodies in relative motion, where the trajectory was determined from the instantaneous aerodynamics. The flow solver and the adaptation scheme were validated by simulating the transonic, unsteady flow around a wing undergoing a forced, periodic pitching motion. Then, to demonstrate the technique and its concept using a typical example for the relative-moving-body problems, the separation of a store from its carriage position under a wing in transonic flight was computationally simulated. Among the noteworthy observations made from the present investigation were the following: 1) The methodology has shown to be accurate, automated, easy for dynamic gridding, and relatively efficient for the required work hours. 2) Determining the trajectory of a free falling object aerodynamically requires a multidisciplinary analysis, using not only adequately accurate but also computationally efficient algorithms. 3) As a cost saving measure, such simulations may be restricted to the duration of the mutual interference effects between the objects. 4) The computational efficiency (by further optimizing the coding and/or implicit time marching[19]) was deemed as the last issue to be investigated before proposing the method for practical and realistic applications.

Acknowledgments

This work was supported by NASA Langley Research Center Grant NAG-1-1499, Technical Monitor J. L. Thomas. The authors also thank N. T. Frink and S. Pirzadeh for their help. This paper was presented at the 6th International Symposium of Computational Fluid Dynamics.

References

[1]Baysal, O., Singh, K. P., and Yen, G.-W., "Dynamic CFD Methods for Prescribed and Aerodynamically-Determined Relative-Moving Multibody Problems," *First AFOSR Conference on Dynamic Motion CFD*, edited by L. Sakell and D. D. Knight, Air Force Office of Scientific Research, Arlington, VA, 1996, pp. 31–44.

[2]Batina, J. T., "Unsteady Euler Airfoil Solutions Using Unstructured Dynamic Meshes," AIAA Paper 89-0115, Jan. 1989.

[3]Baysal, O., and Yen, G. W., "Kinematic Domain Decomposition to Simulate Flows Past Moving Bodies," AIAA Paper 91-0725, Jan. 1991.

[4]Yen, G. W, and Baysal, O., "Computing Unsteady High Speed Flows Past an Oscillating Cylinder Near a Vertical Wall," *Journal of Spacecraft and Rockets*, Vol. 31, No. 4, 1994, pp. 630–635.

[5]Probert, E. J., Hassan, O., and Morgan, K., "An Adaptive Finite Element Method for Transient Compressible Flows with Moving Boundaries," *International Journal for Numerical Methods in Engineering*, Vol. 32, 1991, pp. 751–765.

[6]Kennon, S. R., Meyering, J. M., Berry, C. W., and Oden, J. T., "Geometry Based Delaunay Tetrahedralization and Mesh Movement Strategies for Multibody CFD," *Proceedings of Atmospheric Flight Mechanics Conference*, AIAA, Washington, DC, 1992.

[7]Noack, R. W., and Bishop, D. G., "A Three-Dimensional Delaunay Unstructured Grid Generator and Flow Solver for Bodies in Relative Motion," *Proceedings of Computational Fluid Dynamics Conference*, AIAA, Washington, DC, 1993.

[8]Yen, G. W., and Baysal, O., "Computing Store Separation and Its 6-DOF Trajectory Using 3-D Dynamic Domain Decomposition Method," *Unsteady Flows 1995*, edited by W. L. Keith, H. Tsukamoto, O. Baysal, and T. Wei, FED Vol. 216, American Society of Mechanical Engineers, New York, 1995, pp. 21–28.

[9]Löhner, R., "Adaptive Remeshing for Transient Problems with Moving Bodies," *Proceedings of Atmospheric Flight Mechanics Conference*, AIAA, Washington, DC, 1988.

[10]Singh, K. P., Newman, J. C., III, and Baysal, O., "Dynamic Unstructured Method for Flows Past Multiple Objects in Relative Motion," *AIAA Journal*, Vol. 33, No. 4, 1995, pp. 641–659.

[11]Singh, K. P., and Baysal, O., "Development of a Dynamic Unstructured Euler Method for Moving Rigid Bodies," *Unsteady Flows 1996*, edited by T. Wei, W. L. Keith, and O. Baysal, FED Vol. 312, American Society of Mechanical Engineers, New York, 1996, pp. 32–38.

[12]Singh, K. P., and Baysal, O., "3D Unstructured Method for Flows Past Bodies in 6-DOF Relative Motion," *Proceedings of 6th International Symposium on CFD*, Vol. 3, Univ. of California, Davis, CA, 1995, pp. 1161–1168.

[13]Thomas, P. D., and Lombard, C. K., "Geometric Conservation Law and Its Application to Flow Computations on Moving Grids," *AIAA Journal*, Vol. 17, No. 10, 1979, pp. 1030–1037.

[14]Yen, G. W., and Baysal, O., "Effects of Efficiency Techniques on Accuracy of Dynamic Overlapped Grids for Unsteady Flows," *Journal of Fluids Engineering*, Vol. 119, No. 3, 1997, pp. 577–583.

[15]Frink, N. T., "Upwind Scheme for Solving the Euler Equations on Unstructured Tetrahedral Meshes," *AIAA Journal*, Vol. 30, No. 1, 1992, pp. 70–77.

[16]Heim, E. R., "CFD Wing/Pylon/Finned Store Mutual Interference Wind Tunnel Experiment," Arnold Engineering and Development Center, Rept. AEDC-TSR-91-P4, Tullahoma, TN, Jan. 1991.

[17]Mabey, D. G., Welsh, B. L., and Pyne, C. R., "A Summary of Measurements of Steady and Oscillatory Pressures on a Rectangular Wing," *Aeronautical Journal*, Vol. 92, No. 911, 1988, pp. 10–28.

[18]Chaderjian, N. M., and Guruswamy, G. P., "Transonic Navier–Stokes Computations for an Oscillating Wing Using Zonal Grids," *Journal of Aircraft*, Vol. 29, No. 3, 1992, pp. 326–335.

[19]Baysal, O., and Luo, X.-B., "Dynamic Unstructured Method for Relative Motion of Multi-Body Configuration at Hypersonic Speeds," *Proceedings of 16th AIAA Applied Aerodynamics Conference*, AIAA, Reston, VA, 1998; also *Journal of Aircraft*, Vol. 36, No. 4, 1999, pp. 725–729.

D. S. McRae
Associate Editor